

Rotating mesons in the presence of higher derivative corrections from gauge-string duality

M. Ali-Akbari¹ and K. Bitaghsir Fadafan²

¹*School of Physics, Institute for Research in Fundamental Sciences (IPM)*

P.O.Box 19395-5531, Tehran, Iran

E-mails: aliakbari@theory.ipm.ac.ir

²*Physics Department, Shahrood University of Technology,*

P.O.Box 3619995161, Shahrood, Iran

E-mails: bitaghsir@shahroodut.ac.ir

Abstract

We consider a rotating quark-antiquark ($q\bar{q}$) pair in $\mathcal{N} = 4$ thermal plasma. By using the AdS/CFT correspondence, the properties of this system are investigated. In particular, we study variation of a rotating string radius at the boundary as a function of its tip and angular velocity. We also extend the results to higher derivative corrections *i.e.* \mathcal{R}^2 and \mathcal{R}^4 which correspond to finite coupling corrections on the rotating quark-antiquark system in the hot plasma. In the \mathcal{R}^4 case and for fixed angular velocity the string endpoints become more and more separated as λ^{-1} decreases. To study \mathcal{R}^2 corrections, rotating quark-antiquark system in Gauss-Bonnet background has been considered. We summarize the effects of these corrections in the conclusion section.

1 Introduction

The theory of strong nuclear interactions, QCD, exhibits various phenomena at low energy. These phenomena are strong coupling effects which are not visible in perturbation theory and there are no known quantitative methods to study them (except by lattice simulations). A new method for studying different aspects of strongly coupled gauge theories is the AdS/CFT correspondence [1–5] which has yielded many important insights into the dynamics of strongly coupled gauge theories [6, 7]. Methods based on AdS/CFT relate gravity in AdS_5 space to conformal field theory on the four-dimensional boundary, CFT_4 . It has been shown that an AdS space with a black brane is dual to conformal field theory at finite temperature.

This method is particularly powerful in large N_c gauge theories which are dual to weakly coupled string theories in weakly curved spacetime, since then many computations can be explicitly performed. Although AdS/CFT correspondence is not directly applicable to QCD, one expects that results obtained from closely related non-abelian gauge theories should shed qualitative (or even quantitative) insights into analogous questions in QCD [8, 9]. This has motivated much work devoted to study various properties of thermal SYM theories like the hydrodynamical transport quantities [10].

The experiments of Relativistic Heavy Ion Collisions (RHIC), in which gold nuclei collide at 200 GeV per nucleon, have produced a strongly coupled quark-gluon plasma (QGP) [11]. In order to find out different aspects of QGP and reproduce experimental results, AdS/CFT technology has been used (*e.g.* [12–17]) .

In this paper we study a rotating quark-antiquark pair in $\mathcal{N} = 4$ thermal plasma which can be interpreted as a meson [18]. Based on lattice results and experiments, it is found that the meson shows interesting behavior as the temperature of the plasma increases. It is known that heavy quark bound states can survive in a QGP to temperatures higher than the confinement/deconfinement transition [19]. We use the gauge-string duality [20] to investigate the properties of the above system. Thermal properties of *static* quark-antiquark systems have been studied in [21, 22] in an AdS-Schwarzschild black hole setting using the AdS/CFT correspondence. The static quark-antiquark system is modeled as an open string hanging from the boundary in the bulk (U-shaped string) with its endpoints representing quark and antiquark. The motion of a quark-antiquark pair through $\mathcal{N} = 4$ plasma has been discussed in [23–25]. Several studies of rotating mesons and their related properties have been done in [26–29] by means of the AdS/CFT correspondence. In [30] rotation of a heavy test quark has been considered.

It has been shown that there are two kinds of strings, long strings and short strings, an

analysis of which has shown the stability of the latter kind [31–34]. We show that there are short and long strings in the case of rotating mesons and, based on the stability analysis of binding quark-antiquark pairs, one can show that short strings are more energetically favorable.

We also study the behavior of the radius d of a rotating string at the boundary by plotting d first as a function of the distance between the tip of the U-shaped string and the horizon and then as a function of the string angular velocity ω , the plots of which may be seen in Fig. 2. By a fitting approach, we give a formula for d in terms of ω in (2.18), which describes only physical solutions, *i.e.* short strings. Notice that this result is based on the relation between the tip of the U-shaped string and ω in Fig. 3.

We extend the results to higher derivative corrections which on the gravity side correspond to finite coupling corrections on the gauge theory side. The main motivation to consider corrections comes from the fact that string theory contains higher derivative corrections arising from stringy effects. In the case of $\mathcal{N} = 4$ super Yang-Mills (SYM) theory, the gravity dual corresponds to type IIB string theory on $AdS_5 \times S^5$ background. The leading order correction in $1/\lambda$ arises from stringy correction to the low energy effective action of type IIB supergravity, $\alpha'^3 \mathcal{R}^4$. On the gauge theory side, computations are exactly valid when the 't Hooft coupling constant goes to infinity ($\lambda = g_{YM}^2 N \rightarrow \infty$). An understanding of how these computations are affected by finite λ corrections may be essential for more precise theoretical predictions.

We study \mathcal{R}^4 and \mathcal{R}^2 corrections to the properties of rotating strings by analyzing their shape for a given angular velocity. We find that as λ^{-1} decreases the string endpoints become more and more separated. We also noticed that the radius of a rotating quark-antiquark system is smaller when \mathcal{R}^4 correction is considered. To study \mathcal{R}^2 correction, we consider Gauss-Bonnet (GB) background which is the most general theory of gravity with quadratic powers of curvature in five dimensions. We see that the longer string has more energy than the shorter one and by analyzing Fig. 6 and Fig. 8, we find that the cases with bigger 't Hooft coupling have longer length and therefore more energy. We summarize the effects of these corrections in the last section.

The article is organized as follows. In the next section, we study some properties of rotating open strings in AdS-Schwarzschild black hole extending our analysis to higher derivative corrections in section 3. In the last section we draw our conclusions and summarize our results.

2 Rotating quark-antiquark pair at finite temperature

In this section we study a rotating quark-antiquark system at the boundary as an open string in the bulk space from the gauge-string duality point of view. According to the Maldacena's conjecture, $\mathcal{N} = 4$ $U(N)$ superconformal Yang-Mills theory in $3 + 1$ dimensions is dual to type IIB superstring theory on $AdS_5 \times S^5$ background. The latter background can be realized as a near-horizon geometry of extremal D3-branes in type IIB superstring theory. It is well known that in the large N and strong 't Hooft coupling limit the gauge theory is dual to type IIB supergravity on $AdS_5 \times S^5$.

At finite temperature, the large N and strong coupling limit of $D = 4$ $\mathcal{N} = 4$ SYM theory is dual to the near-horizon geometry of near-extremal D3-branes in IIB superstring theory. This geometry is given by AdS-Schwarzschild type IIB supergravity (when the other compact five-dimensional manifold is S^5)

$$ds^2 = \frac{u^2}{R^2} (-h(u)dt^2 + d\rho^2 + \rho^2 d\theta^2 + dx_3^2) + \frac{du^2}{(\frac{u}{R})^2 h(u)}, \quad (2.1)$$

where

$$h(u) = 1 - \frac{u_h^4}{u^4}. \quad (2.2)$$

Here u is the radial direction which is bounded from below by $u \geq u_h$ where u_h refers to the location of the horizon. The curvature radius of AdS is R . In fact it maps non-perturbative problems at strong coupling onto calculable problems of classical gravity in a five-dimensional AdS_5 black hole spacetime. The temperature in the hot plasma is equal to the Hawking temperature of the AdS black hole in the gravity dual, namely

$$T = \frac{u_h}{\pi R^2}. \quad (2.3)$$

2.1 Rotating quark-antiquark pair as a U-shaped string

In the following we introduce a rotating quark-antiquark pair from string theory and AdS/CFT point of view. In the usual fashion the two endpoints of an open string are seen as a quark and antiquark pair which may be considered as a meson. The open string hanging in the bulk space and connecting two endpoints has a characteristic U-shaped. We name u_* the tip of the U-shaped string and we let it to define the nearest point between the string and the horizon of the black hole ($u_* \geq u_h$). Let us emphasize that for non-physical states we would have $u_* < u_h$ [22].

In order to study a rotating string, we make use of the Nambu-Goto action in the above background given by

$$S = -\frac{1}{2\pi\alpha'} \int d\tau d\sigma \sqrt{-\det g_{ab}}. \quad (2.4)$$

The coordinates (σ, τ) parameterize the induced metric g_{ab} on the string world-sheet. Indices a, b run over the two dimensions of the world-sheet. Let $X^\mu(\sigma, \tau)$ be a map from the string world-sheet into spacetime and let us define $\dot{X} = \partial_\tau X$, $X' = \partial_\sigma X$, and $V \cdot W = V^\mu W^\nu G_{\mu\nu}$ where $G_{\mu\nu}$ is the AdS black hole metric. Indices μ, ν run over the five dimensions of spacetime. Then

$$-g = -\det g_{ab} = (\dot{X} \cdot X')^2 - (X')^2 (\dot{X})^2. \quad (2.5)$$

The background metric is given by (2.1). Our four-dimensional space is along t, ρ, θ and x_3 where the quark-antiquark system is rotating on the ρ, θ plane with x_3 the direction perpendicular to the plane of rotation. We choose to parameterize the two-dimensional world-sheet of the rotating string $X^\mu(\sigma, \tau)$ according to

$$X^\mu(\sigma, \tau) = (t = \tau, \rho = \sigma, u = u(\rho), \theta = \omega t). \quad (2.6)$$

Simply, what this means is that the radius of the rotating quark-antiquark on the probe brane changes with the fifth direction of the bulk space as we move further into the bulk. In arriving at the parametrization (2.6), we made use of the fact that the quark-antiquark pair is in circular motion with radius d at a constant angular velocity ω . Also, we assumed that the system retains its constant circular motion at all times. Furthermore, the ansatz (2.6) does not show any dragging effects which frees us from applying a force to maintain the rigid rotation [28].

In order to describe the rotation of a quark-antiquark pair the end-points of the string on the probe brane must satisfy the following boundary conditions

$$u(d) = \infty, \quad (2.7)$$

$$\frac{\partial u}{\partial \rho} = \infty. \quad (2.8)$$

According to our ansatz (2.6), the Nambu-Goto action with $\alpha' = 1$ becomes

$$S = -\frac{1}{2\pi} \int dt d\rho \sqrt{\left(h(u) - \rho^2 \omega^2\right) \left(\frac{u'^2}{h(u)} + \frac{u^4}{R^4}\right)}, \quad (2.9)$$

where prime is the derivative with respect to ρ . We shall find it convenient to introduce new variables

$$z = \frac{u}{u_h}, \quad \tilde{\rho} = \frac{u_h}{R^2} \rho, \quad \tilde{\omega} = \frac{R^2}{u_h} \omega, \quad (2.10)$$

where in the new variables, prime denotes the derivative with respect to z . Thus we rewrite

the action (2.9) in the new variables as

$$\begin{aligned}
S &= -\frac{u_h}{2\pi} \int dt d\rho \sqrt{(z^4 - 1 - \rho^2 \omega^2 z^4) \left(\frac{z'^2}{z^4 - 1} + 1 \right)} \\
&\equiv -\frac{u_h}{2\pi} \int dt d\rho \mathcal{L}.
\end{aligned} \tag{2.11}$$

where we drop the tildes for convenience. It is evident that positivity of the square root in (2.11) requires that $z^4 - 1 - \rho^2 \omega^2 z^4 \geq 0$. This in turn means that for a given angular velocity ω , the string solution $u(\rho)$ has to lie above the curve

$$u(\rho) \geq \frac{u_h}{(1 - \rho^2 \omega^2)^{1/4}}. \tag{2.12}$$

for its action to be real. It is shown in Fig. 1 that all rotating strings with different angular velocity do satisfy this condition.

The equation of motion for z follows from differentiating the Nambu-Goto action and is given by

$$\partial_\rho \left(\frac{z'(1 - \rho^2 \omega^2 \frac{z^4}{z^4 - 1})}{\sqrt{-g}} \right) - \frac{\partial \mathcal{L}}{\partial z} = 0, \tag{2.13}$$

where

$$\frac{\partial \mathcal{L}}{\partial z} = 2z^3 \left(\frac{(z^4 - 1)^2 + \rho^2 \omega^2 (z'^2 - (z^4 - 1)^2)}{(z^4 - 1)^2 \sqrt{-g}} \right). \tag{2.14}$$

2.2 Numerical solutions

The equation of motion for $z(\rho)$ in (2.13) is nonlinear and coupled. In the simple case of no angular velocity one can reproduce the analysis of the *static* case as given in [21, 22]. However, for generic values of ω we cannot solve this equation analytically and we have to resort to numerical methods.

The boundary conditions which solve (2.13) are

$$z(d) = 20 \quad \text{and} \quad z'(d) \rightarrow \infty. \tag{2.15}$$

Physically (2.15) means that string terminates orthogonally on the brane in the boundary which in turn implies Neumann boundary conditions. Also $z'(0) = 0$ has been considered at the tip of the string where $\rho = 0$. To check the validity of our solutions, we choose $\rho = d$ so that at $\rho = 0$ we keep the condition $z'(0) = 0$.

The shapes of rotating open strings, for a fixed temperature, are shown in Fig. 1. By analyzing the shapes of the string for various angular velocities, we infer that as ω decreases

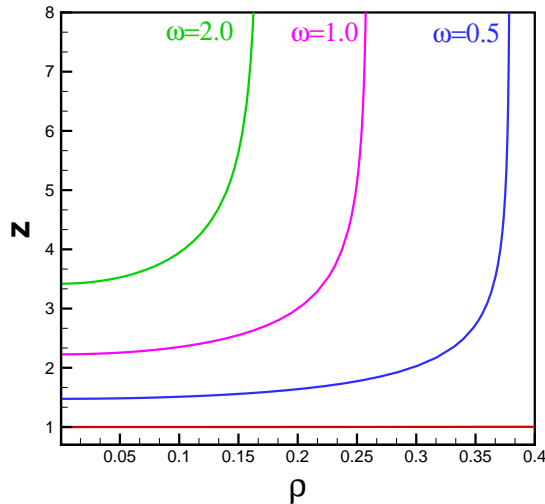


Figure 1: Shapes of open strings for different angular velocities are plotted. All solutions lie above the horizontal line defined by (2.12). Notice that the positivity condition is seen as a straight line at $z = 1$.

the string endpoints become more and more separated, *i.e.* the radius of the open string at the boundary will increase and it will penetrate deeper into the horizon. We would like to stress again that rotating strings with different angular velocities have to lie above the curve given by (2.12) in order their action be real. This is precisely what is shown in Fig. 1.

2.3 Rotating and static quark-antiquark pair

By using numerical solutions, a plot of d as a function of angular velocity ω is given in Fig. 2 where it is seen that both ω and d increase up to a maximum. As ω increases and goes past its maximum the radius of the rotating open string decreases. Hence there are two possible U-shaped configurations representing two different values of ω . However, only the right region of the plots is physical where to an increasing ω there corresponds a decreasing radius. The configurations with larger values of ω have shorter length and hence more energetically favorable. Therefore the branch to the left of the maximum in Fig. 2. is presumably unstable and will decay to the right branch.

It is interesting to investigate the behavior of a rotating quark-antiquark pair in terms of the strings tip. To this end, we introduce a new parameter $a = \frac{u_*}{u_h}$ where u_* is the nearest point of the (physical) string to the horizon. In the right plot of Fig. 2 we show d versus a . In the physical region, as a increases the value of d decreases. It is obvious that there are two possible U-shaped string configurations at two different values of a . The larger value of a has shorter length and hence it describes physical configurations. In order to check the

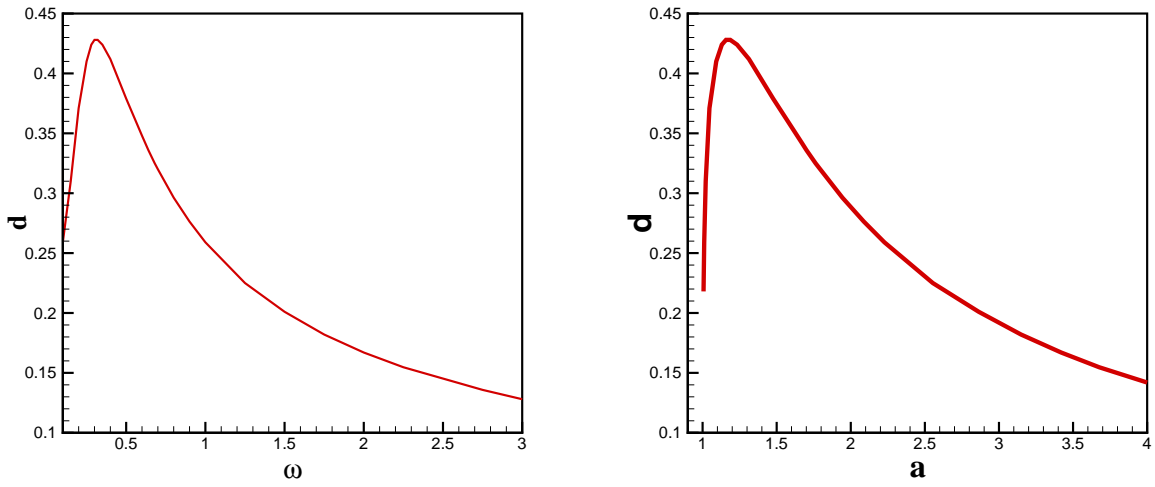


Figure 2: Left: The radius of a rotating quark-antiquark at the boundary versus the angular velocity. Right: The radius of a rotating quark-antiquark at the boundary versus a .

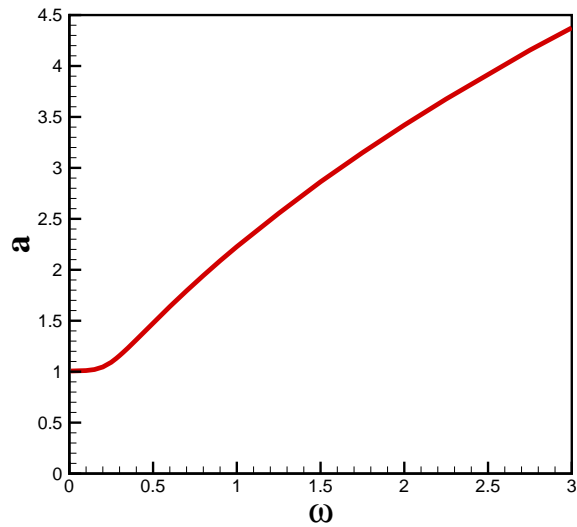


Figure 3: We plot a versus angular velocity ω .

behavior of angular velocity ω in terms of a , we plot them in Fig. 3. In the physical region, angular velocity ω is approximately a linear function of a . We fit this linear curve using

$$a = m + n\omega + p\omega^2. \quad (2.16)$$

A numerical analysis of (2.16) gives optimal values $m = 0.70$, $n = 1.65$ and $p = -0.14$. The d - a curve is also fitted by

$$d(a) = \frac{s}{a} + \frac{r}{a^5}, \quad (2.17)$$

where $s = 0.57$ and $r = -0.01$. The d - ω curve is easily found by substituting (2.16) in (2.17)

$$d(\omega) = \frac{0.57}{0.70 + 1.65\omega - 0.14\omega^2} - \frac{0.01}{(0.70 + 1.65\omega - 0.14\omega^2)^5}, \quad (2.18)$$

which reproduces the d - ω plot in Fig. 2. It is important to notice that d and a are always positive and thus we have an upper limit on ω . Without the third term in (2.16), a and d are always positive and ω is free to go to infinity. We draw the reader's attention to the fact that in the physical region ω cannot be zero.

In [22] the heavy *static* quark-antiquark potential as a function of interquark distance d was defined. It was argued that at the particular point $d = d_*$ the potential curve crosses zero. Gauge-string duality implies that the U-shaped string will break into two straight open strings having no interaction energy and vanishing potential for $d \geq d_*$. Furthermore, in the same paper the relation between d and a was also considered. There, two possible U-shaped string configurations at two different values of a arise. In the physical region, as a increases the value of d decreases. In addition, for large a , d was obtained as a function of a

$$d(a) = \frac{2c\lambda}{u_h} \left(\frac{1}{a} - \frac{1}{5a^5} - \frac{1}{10a^9} - \dots \right), \quad (2.19)$$

where $c = 0.56$.

In the our case we have plotted the radius of a rotating quark-antiquark system in terms of a and in comparison with static case we find similar curves which we reproduce in Fig. 4. One may conclude that the behavior of d as a function of a is the same as in the static case (2.19), where the coefficients depend on angular velocity. In other words for large a we may have

$$d(a) = \frac{2c\lambda}{u_h} \left(\frac{\alpha(\omega)}{a} - \frac{\beta(\omega)}{5a^5} - \frac{\gamma(\omega)}{10a^9} - \dots \right), \quad (2.20)$$

where

$$\alpha(\omega = 0) = \beta(\omega = 0) = \gamma(\omega = 0) = 1. \quad (2.21)$$

It would be interesting to find values for α , β and γ [35].

Moreover it is clear that angular velocity is responsible for both the variation of the radius of the quark-antiquark system as well as a , see Fig. 3. Similarly to our discussion of the potential in the static case, we find that in the *rotating* case for a particular value ω_* such that $\omega_* > \omega_{max}$, corresponding to $d_* < d_{max}$, dissociation appears. Once dissociation has appeared we are left with a pair of straight strings whose potential vanishes for $\omega < \omega_*$ ($d > d_*$).

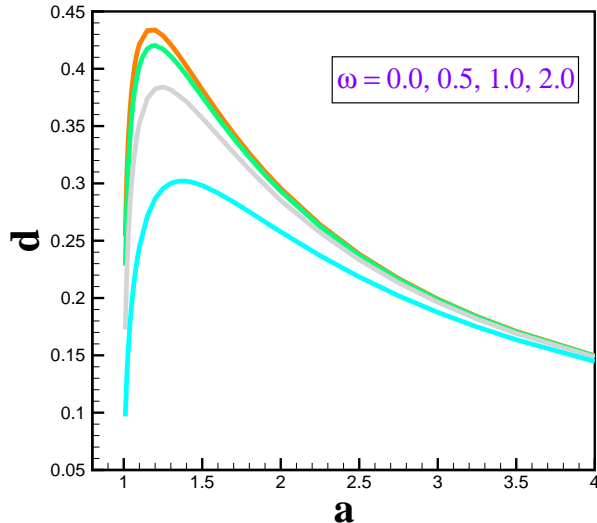


Figure 4: We plot d versus a for different values of angular velocity of the quark-antiquark pair. From maximum d to minimum d , angular velocity is $w = 0.0, 0.5, 1.0, 2.0$. In this figure we have fixed angular velocity of the rotating string. Also we have not considered Neumann boundary conditions (boundary is located at $z=20$). See the similarity with rotating baryon in Figure 5 of [37].

A string-junction holographic model of a probe baryon in finite temperature SYM dual to AdS-Schwarzschild black hole is studied in [36–38]. Therein, a relation between D5-brane position, which plays the same role of a of the U-shaped string in our work, and quark separation is plotted. It was shown that quark separation becomes larger at first to turn smaller as the position of the D5-brane increases. It was argued that in the physical region by increasing the position of the D5-brane the quark separation decreases. Interestingly, it was also discussed that to an increase of the angular velocity there corresponds a decrease of the maximum height of quark separation. Importantly, they did not consider Neumann boundary conditions in this case. Since the results match ours we may conclude that in our case the maximum height of the radius of the quark-antiquark system depends on angular velocity. On the other hand, the ω dependence of α , β and γ should control the height of the maximum [35]. In order to verify the above guess at least numerically we do not

consider boundary conditions and we plot in Fig. 4 quark-antiquark separation in terms of a for different angular velocities. It is easy to see that by increasing angular velocity the maximum value of d decreases.

2.4 Dissociation of rotating quark-antiquark pair

In this subsection, we analyze the dissociation of a rotating quark-antiquark pair. This subject has been studied in [28, 29]. As we found in the previous section angular velocity controls the radius, the length and the nearest point of the string to the horizon. We are going to understand the effect of rotation on the dissociation of a rotating quark-antiquark pair by studying the energy E and angular momentum J . These are constants of motion and they can be easily found from the action (2.11). The angular momentum of the quark-antiquark is

$$J = \omega \int d\rho \rho^2 z^4 \left(\frac{z'^2}{z^4 - 1} + 1 \right) \frac{1}{\sqrt{-g}}. \quad (2.22)$$

The other constant is the energy of the system that follows from the Hamiltonian

$$\mathcal{H} = \dot{\theta} \frac{\partial \mathcal{L}}{\partial \dot{\theta}} - \mathcal{L}, \quad (2.23)$$

and it can be found to be

$$E = \int d\rho \frac{z'^2 + z^4 - 1}{\sqrt{-g}}. \quad (2.24)$$

It is not easy to find analytical solutions for $E(\omega)$ and $J(\omega)$, so we resort to numerical analysis to obtain more information about these quantities. The results are shown in Fig. 5 where we plotted the energy squared of the rotating quark-antiquark pair in terms of its angular momentum. Horizon and boundary are located at $z_h = 1$ and $z = 20$, respectively. From the upper curve to the lower curve we see that temperature increases. From equation (2.3) it is clear that a change in temperature corresponds to a change in the location of the horizon. There is a maximum energy and angular velocity beyond which the meson will dissociate.

At finite temperature, as ω decreases, the effective tension of the string in the region near the horizon decreases. This leads to the appearance of a maximum in energy and spin. It is natural to interpret the temperature at which this happens as the critical temperature at which a quark-antiquark of spin J_{max} melts. Thus we deduce that the dissociation temperature for quark-antiquark is spin dependent. As temperature increases the maximum value of the spin that a quark-antiquark can carry decreases, see Fig 5. Moreover, we see that two states with identical spin have different energies. The ones with smaller ω are more energetic than the ones with larger ω . This entails that larger values of ω are more stable.

We eliminate the variable ω from the equations for energy and spin to obtain a plot of energy versus spin shown in Fig. 5.

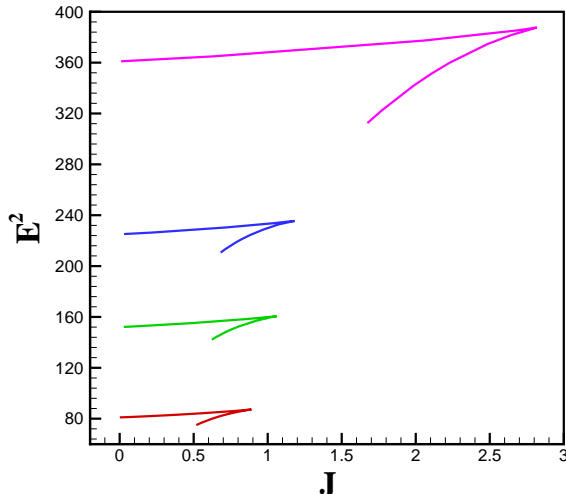


Figure 5: The energy squared of a rotating string is plotted versus angular momentum. From the upper curve to the lower curve, temperature is increasing which corresponds to $z_h = 1, 1.25, 1.50, 2.0$.

3 Finite coupling corrections and rotating $q\bar{q}$ pair

Let us now study finite coupling corrections to the rotating quark-antiquark pair by considering \mathcal{R}^2 and \mathcal{R}^4 corrections in the dual gravity background. We should emphasize that in the case of \mathcal{R}^2 correction, one cannot predict a result for $\mathcal{N} = 4$ SYM because the first higher derivative correction in weakly curved type IIB backgrounds enters at order \mathcal{R}^4 . These corrections on the drag force have been studied in [39].

We follow the same procedure as in the previous section and start with the Nambu-Goto action in these two different backgrounds. We will see, as it is expected, results for \mathcal{R}^4 correction are almost similar to AdS-Schwarzschild black hole without correction studied in the previous section.

3.1 \mathcal{R}^4 corrections to AdS-Schwarzschild black brane

We begin by studying a rotating string in the α' corrected background. As before we will write the Nambu-Goto action and then discuss the different aspects of rotating strings.

Since AdS/CFT correspondence refers to complete string theory, one should consider the string corrections to the 10D supergravity action. The first correction occurs at order

$(\alpha')^3$ [40]. In the extremal $AdS_5 \times S^5$ it is clear that the metric does not change [41], conversely this is no longer true in the non-extremal case. Corrections in inverse 't Hooft coupling $1/\lambda$ which correspond to α' corrections on the string theory side were found in [42]. The α' -corrected metric is [43]

$$ds^2 = G_{tt} dt^2 + G_{xx}(d\rho^2 + \rho^2 d\theta^2 + dx_3^2) + G_{uu} du^2, \quad (3.1)$$

where the metric functions are given by

$$\begin{aligned} G_{tt} &= -R^{-2}u^2(1 - z^{-4})T(z), \\ G_{xx} &= R^{-2}u^2X(z), \\ G_{uu} &= R^2u^{-2}(1 - z^{-4})^{-1}U(z), \end{aligned} \quad (3.2)$$

and

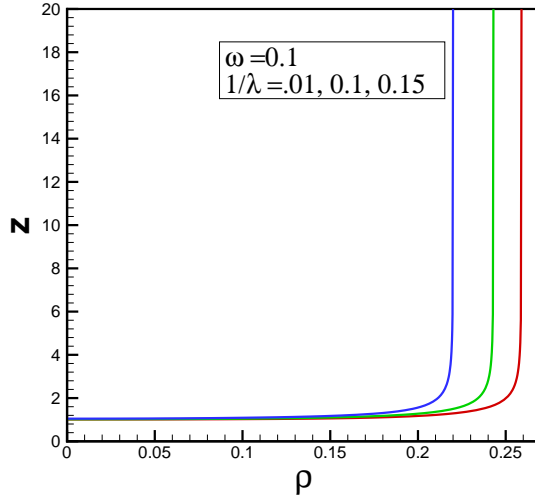


Figure 6: Shape of a rotating string for different values of λ^{-1} at fixed angular velocity $\omega = 0.1$. From right to left $\lambda^{-1} = 0.01, 0.1, 0.15$

$$\begin{aligned} T(z) &= 1 - b \left(75z^{-4} + \frac{1225}{16}z^{-8} - \frac{695}{16}z^{-12} \right) + \dots, \\ X(z) &= 1 - \frac{25b}{16}z^{-8}(1 + z^{-4}) + \dots, \\ U(z) &= 1 + b \left(75z^{-4} + \frac{1175}{16}z^{-8} - \frac{4585}{16}z^{-12} \right) + \dots \end{aligned} \quad (3.3)$$

There is an event horizon at $u = u_h$ and the geometry is asymptotically AdS at large u with a radius of curvature R . The expansion parameter b can be expressed in terms of the inverse

't Hooft coupling as

$$b = \frac{\zeta(3)}{8} \lambda^{-3/2} \sim .15 \lambda^{-3/2}. \quad (3.4)$$

The dynamics of a rotating string in this background is described by the Nambu-Goto action

$$S = -\frac{u_h}{2\pi} \int dt d\rho \sqrt{\left((z^4 - 1)T(z) - \rho^2 \omega^2 z^4 X(z) \right) \left(\frac{z'^2}{z^4 - 1} U(z) + X(z) \right)}, \quad (3.5)$$

where, in deriving (3.5), we used (2.6) and (2.10). The positivity condition becomes

$$(z^4 - 1)T(z) \geq \rho^2 \omega^2 z^4 X(z). \quad (3.6)$$

One can easily find equation of motion for z and then solve it numerically leading to Fig. 6. In this figure, for fixed ω , a plot of $z(\rho)$ versus ρ is depicted. By analyzing the shapes of the string for various values of λ^{-1} we see that as λ^{-1} decreases the separation of the string endpoints increases.

For fixed λ^{-1} , as shown in Fig. 7, we again have physical and unphysical strings. For physical strings, as angular velocity decreases the rotating string endpoints become more separated and the U-shaped string penetrates deeper into the horizon. One can compare Fig. 7 with previous results in the case of no corrections. It is clear that the distance between rotating quark and antiquark is smaller when \mathcal{R}^4 correction is considered.

It would be interesting to connect this result to experiments at RHIC and LHC. Thermal properties of QGP can be investigated by quarkonium states. The suppression of heavy quark bound states in RHIC is a sensitive probe for QGP. Quarkonium is a bound state of a heavy quark and antiquark pair and it is possible to introduce screening length for it. When the screening radius is smaller than the radius of the bound state quarkonium will dissociate. Then by studying this physical quantity one can find the effect of finite coupling corrections on the dissociation of charmonium and bottomonium at RHIC. This can be done in detail by studying the potential of the rotating quark-antiquark and we leave this problem for further study [35].

Since the \mathcal{R}^4 correction has a small effect on other results of the previous section we do not repeat them.

3.2 Gauss-Bonnet gravity background

We continue our analysis and consider \mathcal{R}^2 correction. On the gravity side it corresponds to finite coupling correction on the gauge theory side. Motivation to consider this correction comes from the fact that string theory contains higher derivative corrections from stringy ($1/\lambda$) or quantum effects ($1/N$). In other words, a possible violation of the lower bound of the

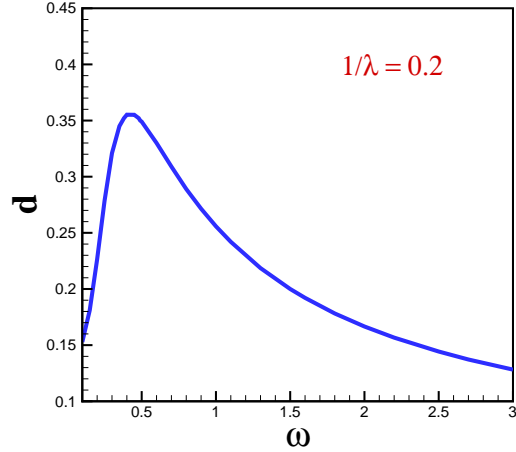


Figure 7: The radius of a rotating meson versus the angular velocity for fixed coupling, $\lambda^{-1} = 0.2$.

ratio of shear viscosity η to entropy density s in GB background was shown in [46, 48], also see [47] and references therein. Following this observation, we study properties of rotating quark-antiquark in GB gravity.

In five dimensions, the most general theory of gravity with quadratic powers of curvature and exact solution is Einstein-Gauss-Bonnet (EGB) theory which is defined by the following action [44]

$$S = \frac{1}{16\pi G_N} \int d^5x \sqrt{-g} \left(\mathcal{R} + \frac{12}{R^2} + \frac{\lambda_{GB} R^2}{2} (\mathcal{R}^2 - 4\mathcal{R}_{\mu\nu}\mathcal{R}^{\mu\nu} + \mathcal{R}^{\mu\nu\alpha\beta}\mathcal{R}_{\mu\nu\alpha\beta}) \right). \quad (3.7)$$

Here R is proportional to the radius of the asymptotic AdS space and μ runs over 1 to 5. We are going to consider how curvature squared terms affect rotating strings. There is an exact black brane solution whose metric is of the form (3.1) with [45]

$$G_{tt} = -kR^{-2}u^2h(u), \quad G_{xx} = R^{-2}u^2, \quad G_{uu} = R^2u^{-2}h^{-1}(u), \quad (3.8)$$

where

$$h(u) = \frac{1}{2\lambda_{GB}} \left[1 - \sqrt{1 - 4\lambda_{GB} \left(1 - \frac{u_h^4}{u^4} \right)} \right], \quad k = \frac{1}{2} (1 + \sqrt{1 - 4\lambda_{GB}}). \quad (3.9)$$

The scaling factor k for G_{tt} ensures us that the speed of light at the boundary theory is one. Beyond $\lambda_{GB} \leq \frac{1}{4}$ there is no vacuum AdS solution and one cannot have a conformal field theory at the boundary. New bounds for λ_{GB} come from causality condition. Authors of [48] found that in five dimensions $\lambda_{GB} \leq 0.09$ and when dimensions of spacetime go up,

causality restricts the value of λ_{GB} in the region $\lambda_{GB} \leq 0.25$. The Hawking temperature of the black hole is given by

$$T = \frac{\sqrt{k} u_h}{\pi R^2}. \quad (3.10)$$

Using (2.6) and (2.10), the Nambu-Goto action becomes

$$\begin{aligned} S &= -\frac{u_h}{2\pi} \int dt d\rho \sqrt{(kh(z) - \rho^2\omega^2)(z^4 + z'^2 h^{-1}(z))} \\ &\equiv -\frac{u_h}{2\pi} \int dt d\rho \mathcal{L}, \end{aligned} \quad (3.11)$$

where

$$h(z) = \frac{1}{2\lambda_{GB}} \left[1 - \sqrt{1 - 4\lambda_{GB}(1 - z^{-4})} \right]. \quad (3.12)$$

Positivity of the square root in the action leads to

$$u(\rho) \geq \frac{u_h}{\left(1 - \frac{1}{4\lambda_{GB}} \left(1 - \left(1 - \frac{2\lambda_{GB}}{k} \rho^2 \omega^2 \right)^2 \right) \right)^{1/4}}. \quad (3.13)$$

Equation (3.13) implies that rotating strings have to lie above this curve. The equation of

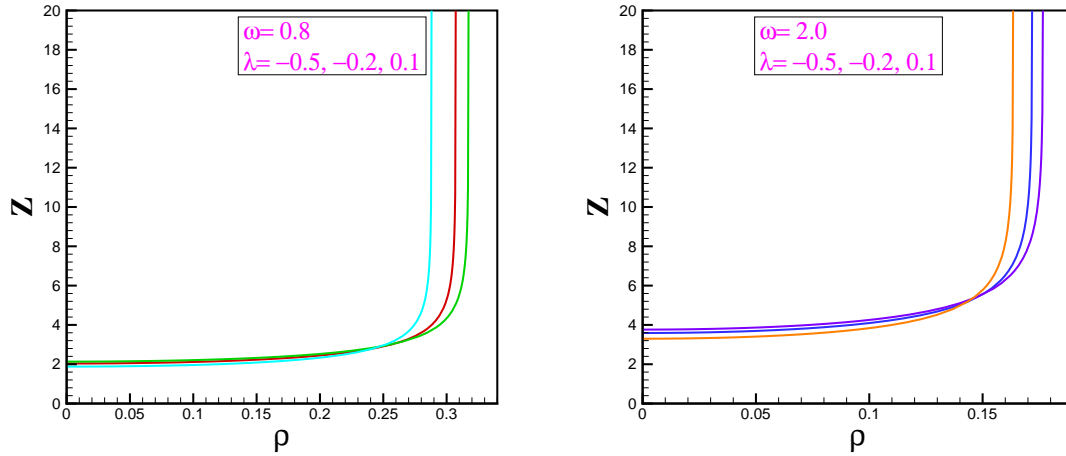


Figure 8: Shapes of a rotating heavy meson for different values of coupling constants. Left: For $\omega = 0.8$ coupling constants $\lambda_{GB} = -0.5, -0.2, 0.1$ from the right to the left curve. Right: For $\omega = 2.0$ coupling constants $\lambda_{GB} = -0.5, -0.2, 0.1$ from the right to the left curve.

motion for z is

$$\partial_\rho \left(\frac{z' h^{-1}(z) (kh(z) - \rho^2 \omega^2)}{\sqrt{-g}} \right) - \frac{\partial \mathcal{L}}{\partial z} = 0. \quad (3.14)$$

One can solve this equation numerically to obtain more information about a rotating quark-antiquark pair in the EGB background. Boundary conditions which solve the differential

equation (3.14) are $z(d) = 20$ and $z'(d) \rightarrow \infty$. Also the condition $z'(0) = 0$ at the tip of the string is employed. The shapes of rotating open string, for fixed temperature and different angular velocities and λ_{GB} are shown in Fig. 8. By analyzing the shapes of the string for different values of λ_{GB} with fixed ω , as λ_{GB} increases the string endpoints become more separated *i.e.* the radius d of the rotating open string at the boundary increases but the tip of the U-shaped string does not change considerably. Also it is evident that shorter strings, *i.e.* smaller d , have larger angular velocities which similarly to our previous cases. Comparing the two plots in Fig. 8, we realize that for larger angular velocities there corresponds smaller radii of the quark-antiquark system.

3.2.1 Energy and spin

The spin and energy of a quark-antiquark in the above background are easily defined by

$$\begin{aligned} J &= \omega \int d\rho \rho^2 \left(\frac{z^4 + z'^2 h^{-1}(z)}{\sqrt{-g}} \right), \\ E &= k \int d\rho \frac{h(z)(z^4 + z'^2 h^{-1}(z))}{\sqrt{-g}}. \end{aligned} \tag{3.15}$$

Energy squared in terms of spin is plotted in Fig. 9. It is evident that like in previous cases there is a maximum which may be related to a dissociation point. The maximum of the energy squared is noticeably enhanced respect to prior cases. Also, the effect of the GB coupling is seen in the same figure whereby an increase of λ_{GB} yields a decrease of the maximum energy and spin. This is an interesting phenomenon that shows us the role of finite coupling corrections. If we compare it with the case of no corrections, a rotating meson will dissociate with smaller energy and spin.

4 Conclusion

In this paper we studied a rotating quark-antiquark in AdS-Schwarzschild black hole and solved its equation of motion numerically. By using suitable boundary conditions, at fixed temperature, we find two U-shaped strings of which the shorter one is energetically stable. By analyzing string shapes, corresponding to physical regions, we deduce that as angular velocity decreases (*i.e.* a decreases) the string endpoints become more separated, that is the radius of the rotating string at the boundary increases. Interestingly, our results match with a similar analysis carried out in Sakai-Sugimoto model [28]. In addition, in (2.16) we were able to cast an equation which expresses the distance between the tip of the rotating open string and the horizon in terms of angular velocity. The upper limit on angular velocity comes from the positivity of d .

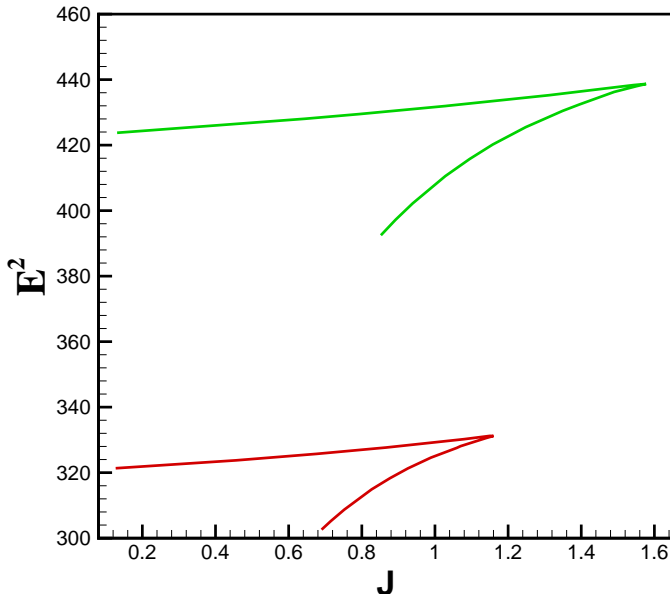


Figure 9: The energy squared of rotating string in terms of the spin in hot plasma dual to Gauss-Bonnet gravity. $u_h = 1$ and boundary is located at $u = 20$. For upper curve $\lambda_{GB} = -0.2$ and for lower curve $\lambda_{GB} = +0.1$. It is clear that there is a maximum energy and spin where beyond them the meson will be dissociated.

Our study has lead us to equation (2.20) which describes the radius of a rotating quark-antiquark in terms of a and ω where remarkably the dependence on a is exactly as for the static case. We plan to derive the α, β and γ functions appearing in (2.20) in a future work [35]. This can be done by either best fitting methods or analytically as in [22]. We also found a similarity between our setting and the baryonic case. We showed that the tip of the string in our model and the position of a D5-brane in the baryonic case play the same role: by increasing angular velocity both of them behave alike.

By plotting energy in terms of spin we showed that at a fixed temperature spin has a maximum value interpreted as a temperature-dependent dissociation spin.

We also extended our setup as to include \mathcal{R}^2 and \mathcal{R}^4 corrections. We summarize our results as follows:

- The effects of \mathcal{R}^4 higher order correction can be controlled by λ^{-1} . For a fixed ω , by increasing λ^{-1} the radius of the rotating open string increases although the tip of the string is almost constant. In other words, in presence of higher order correction the rotating open string has longer length. Since the longer string is more energetic we conclude that the \mathcal{R}^4 correction increases the value of energy. In short, the radius, length and energy of a rotating open string will increase when \mathcal{R}^4 correction becomes

bigger. We showed that \mathcal{R}^2 correction yields the same results as \mathcal{R}^4 correction does.

- As the potential between a quark and antiquark becomes zero, a free quark and antiquark are produced. In the case of a rotating open string it happens when $d = d_*(\omega = \omega_*)$. Because of \mathcal{R}^4 correction the value of ω_* decreases which indicates that the quark-antiquark system can be separated more easily than before.
- We considered \mathcal{R}^2 correction in GB theory and found that there is a sensible enhancement in energy.

We conclude with a final remark. Finite coupling corrections may be useful to study the dissociation of quarkonium at RHIC. From this point of view our results can be interpreted as melting of quarkonium states.

Acknowledgment

We would like to thank J. Sonnenschein and K. Hashimoto for their helpful comments and especially thank M. Edalati for reading the manuscript and valuable discussion. It is also a pleasure to thank M. Vincon for reading the manuscript carefully.

References

- [1] O. Aharony, S. S. Gubser, J. M. Maldacena, H. Ooguri and Y. Oz, “Large N field theories, string theory and gravity,” *Phys. Rep.* **323**, 183 (2000) [arXiv:hep-th/9905111];
- [2] J. M. Maldacena, “The large N limit of superconformal field theories and supergravity,” *Adv. Theor. Math. Phys.* **2** (1998) 231 [*Int. J. Theor. Phys.* **38** (1999) 1113] [arXiv:hep-th/9711200]; S. J. Rey and J. T. Yee, “Macroscopic strings as heavy quarks in large N gauge theory and anti-de Sitter supergravity,” *Eur. Phys. J. C* **22** (2001) 379 [arXiv:hep-th/9803001].
- [3] S. S. Gubser, I. R. Klebanov and A. M. Polyakov, “Gauge theory correlators from non-critical string theory,” *Phys. Lett. B* **428** (1998) 105 [arXiv:hep-th/9802109];
- [4] E. Witten, “Anti-de Sitter space and holography,” *Adv. Theor. Math. Phys.* **2** (1998) 253 [arXiv:hep-th/9802150];
- [5] E. Witten, “Anti-de Sitter space, thermal phase transition, and confinement in gauge theories,” *Adv. Theor. Math. Phys.* **2** (1998) 505 [arXiv:hep-th/9803131];

- [6] K. Peeters and M. Zamaklar, “The string/gauge theory correspondence in QCD,” *Eur. Phys. J. ST* **152** (2007) 113 [arXiv:0708.1502 [hep-ph]].
- [7] D. Mateos, “String Theory and Quantum Chromodynamics,” *Class. Quant. Grav.* **24** (2007) S713 [arXiv:0709.1523 [hep-th]].
- [8] J. D. Edelstein, J. P. Shock and D. Zoakos, “The AdS/CFT Correspondence and Non-perturbative QCD,” *AIP Conf. Proc.* **1116** (2009) 265 [arXiv:0901.2534 [hep-ph]].
- [9] R. C. Myers and S. E. Vazquez, “Quark Soup al dente: Applied Superstring Theory,” *Class. Quant. Grav.* **25** (2008) 114008 [arXiv:0804.2423 [hep-th]].
- [10] S. S. Gubser, “Using string theory to study the quark-gluon plasma: progress and perils,” arXiv:0907.4808 [hep-th].
- [11] E. V. Shuryak, “What RHIC experiments and theory tell us about properties of quark-gluon Nucl. Phys. A **750** (2005) 64 [arXiv:hep-ph/0405066]; K. Adcox *et al.* [PHENIX Collaboration], “Formation of dense partonic matter in relativistic nucleus collisions at RHIC: Experimental evaluation by the PHENIX collaboration,” *Nucl. Phys. A* **757** (2005) 184 [arXiv:nucl-ex/0410003]; I. Arsene *et al.* [BRAHMS Collaboration], “Quark gluon plasma and color glass condensate at RHIC? The perspective from the BRAHMS experiment,” *Nucl. Phys. A* **757** (2005) 1 [arXiv:nucl-ex/0410020]; J. Adams *et al.* [STAR Collaboration], “Experimental and theoretical challenges in the search for the quark gluon plasma: The STAR collaboration’s critical assessment of the evidence from RHIC collisions,” *Nucl. Phys. A* **757** (2005) 102 [arXiv:nucl-ex/0501009]; M. Panero, “Thermodynamics of the QCD plasma and the large-N limit,” *Phys. Rev. Lett.* **103** (2009) 232001 [arXiv:0907.3719 [hep-lat]].
- [12] H. Liu, K. Rajagopal and U. A. Wiedemann, “An AdS/CFT calculation of screening in a hot wind,” *Phys. Rev. Lett.* **98** (2007) 182301 [arXiv:hep-ph/0607062].
- [13] H. Liu, K. Rajagopal and U. A. Wiedemann, “Calculating the jet quenching parameter from AdS/CFT,” *Phys. Rev. Lett.* **97** (2006) 182301 [arXiv:hep-ph/0605178].
- [14] C. P. Herzog, A. Karch, P. Kovtun, C. Kozcaz and L. G. Yaffe, “Energy loss of a heavy quark moving through $N = 4$ supersymmetric Yang-Mills plasma,” *JHEP* **0607** (2006) 013 [arXiv:hep-th/0605158].
- [15] J. Casalderrey-Solana and D. Teaney, “Heavy quark diffusion in strongly coupled $N = 4$ Yang-Mills,” *Phys. Rev. D* **74** (2006) 085012 [arXiv:hep-ph/0605199].

- [16] S. S. Gubser, “Drag force in AdS/CFT,” *Phys. Rev. D* **74** (2006) 126005 [arXiv:hep-th/0605182].
- [17] S. S. Gubser, “Comparing the drag force on heavy quarks in $N = 4$ super-Yang-Mills theory and QCD,” *Phys. Rev. D* **76** (2007) 126003 [arXiv:hep-th/0611272].
- [18] J. Erdmenger, N. Evans, I. Kirsch and E. Threlfall, “Mesons in Gauge/Gravity Duals - A Review,” *Eur. Phys. J. A* **35** (2008) 81 [arXiv:0711.4467 [hep-th]].
- [19] P. de Forcrand *et al.* [QCD-TARO Collaboration], “Meson correlators in finite temperature lattice QCD,” *Phys. Rev. D* **63** (2001) 054501 [arXiv:hep-lat/0008005].
- [20] S. S. Gubser and A. Karch, “From gauge-string duality to strong interactions: a Pedestrian’s Guide,” arXiv:0901.0935 [hep-th].
- [21] J. M. Maldacena, “Wilson loops in large N field theories,” *Phys. Rev. Lett.* **80** (1998) 4859 [arXiv:hep-th/9803002].
- [22] S. J. Rey, S. Theisen and J. T. Yee, “Wilson-Polyakov loop at finite temperature in large N gauge theory and anti-de Sitter supergravity,” *Nucl. Phys. B* **527**, 171 (1998) [arXiv:hep-th/9803135];
- [23] M. Chernicoff, J. A. Garcia and A. Guijosa, “The energy of a moving quark-antiquark pair in an $N = 4$ SYM plasma,” *JHEP* **0609** (2006) 068 [arXiv:hep-th/0607089].
- [24] P. C. Argyres, M. Edalati and J. F. Vazquez-Poritz, “No-drag string configurations for steadily moving quark-antiquark pairs in a thermal bath,” *JHEP* **0701** (2007) 105 [arXiv:hep-th/0608118].
- [25] J. Sadeghi, B. Pourhassan and S. Heshmatian, “Drag Force on Rotating Quark-Antiquark Pair in a $N=4$ SYM plasma,” arXiv:0812.4816 [hep-th].
- [26] M. Kruczenski, D. Mateos, R. C. Myers and D. J. Winters “Meson spectroscopy in AdS/CFT with flavour,” *JHEP* **0307** (2003) 049 [arXiv:hep-th/0304032];
- [27] M. Kruczenski, L. A. P. Zayas, J. Sonnenschein and D. Vaman, “Regge trajectories for mesons in the holographic dual of large- $N(c)$ QCD,” *JHEP* **0506** (2005) 046 [arXiv:hep-th/0410035];
- [28] K. Peeters, J. Sonnenschein and M. Zamaklar, “Holographic melting and related properties of mesons in a quark gluon plasma,” *Phys. Rev. D* **74** (2006) 106008 [arXiv:hep-th/0606195];

- [29] O. Antipin, P. Burikham and J. Li, “Effective Quark Antiquark Potential in the Quark Gluon Plasma from Gravity Dual Models,” *JHEP* **0706** (2007) 046 [arXiv:hep-ph/0703105]; P. Burikham and J. Li, “Aspects of the screening length and drag force in two alternative gravity duals of the quark-gluon plasma,” *JHEP* **0703**, 067 (2007) [arXiv:hep-ph/0701259];
- [30] K. B. Fadafan, H. Liu, K. Rajagopal and U. A. Wiedemann, “Stirring Strongly Coupled Plasma,” *Eur. Phys. J. C* **61** (2009) 553 [arXiv:0809.2869 [hep-ph]].
- [31] J. J. Friess, S. S. Gubser, G. Michalogiorgakis and S. S. Pufu, “Stability of strings binding heavy-quark mesons,” *JHEP* **0704** (2007) 079 [arXiv:hep-th/0609137].
- [32] S. D. Avramis, K. Sfetsos and K. Siampos, “Stability of strings dual to flux tubes between static quarks in N=4 SYM,” *Nucl. Phys. B* **769** (2007) 44 [arXiv:hep-th/0612139].
- [33] S. D. Avramis, K. Sfetsos and K. Siampos, “Stability of string configurations dual to quarkonium states in AdS/CFT,” *Nucl. Phys. B* **793** (2008) 1 [arXiv:0706.2655 [hep-th]].
- [34] K. Sfetsos and K. Siampos, “Stability issues with baryons in AdS/CFT,” *JHEP* **0808** (2008) 071 [arXiv:0807.0236 [hep-th]].
- [35] M. Ali-Akbari, K. Bitaghsir, ”Work in progress”
- [36] C. Athanasiou, H. Liu and K. Rajagopal, “Velocity Dependence of Baryon Screening in a Hot Strongly Coupled Plasma,” *JHEP* **0805** (2008) 083 [arXiv:0801.1117 [hep-th]].
- [37] M. Li, Y. Zhou and P. Pu, “High spin baryon in hot strongly coupled plasma,” *JHEP* **0810**, 010 (2008) [arXiv:0805.1611 [hep-th]];
- [38] S. J. Sin and Y. Zhou, “Holographic melting of Heavy Baryons in Plasma with Gluon Condensation,” arXiv:0904.4249 [hep-th]. C. Krishnan, “Baryon Dissociation in a Strongly Coupled Plasma,” *JHEP* **0812** (2008) 019 [arXiv:0809.5143 [hep-th]].
- [39] K. B. Fadafan, “Medium effect and finite ’t Hooft coupling correction on drag force and Jet Quenching Parameter,” arXiv:0809.1336 [hep-th]. K. B. Fadafan, “ R^2 curvature-squared corrections on drag force,” *JHEP* **0812** (2008) 051 [arXiv:0803.2777 [hep-th]]. J. F. Vazquez-Poritz, “Drag force at finite ’t Hooft coupling from AdS/CFT,” [arXiv:0803.2890 [hep-th]];
- [40] M.T. Grisaru and D. Zanon, *Phys. Lett B* **177** (1996) 347;

- [41] T. Banks and M. B. Green, “Non-perturbative effects in AdS(5) x S**5 string theory and d = 4 SUSY Yang-Mills,” JHEP **9805**, 002 (1998) [arXiv:hep-th/9804170];
- [42] J. Pawelczyk and S. Theisen, *AdS₅ × S⁵ black hole metric at O(α’³)*, JHEP **9809** (1998) 010, [hep-th/9808126];
- [43] S.S. Gubser, I.R. Klebanov and A.A. Tseytlin, *Coupling constant dependence in the thermodynamics of N = 4 supersymmetric Yang-Mills theory* Nucl. Phys. **B534** (1998) 202, [hep-th/9805156];
- [44] B. Zwiebach, “Curvature Squared Terms And String Theories,” Phys. Lett. B **156**, 315 (1985).
- [45] R. G. Cai, “Gauss-Bonnet black holes in AdS spaces,” Phys. Rev. D **65**, 084014 (2002) [arXiv:hep-th/0109133];
- [46] Y. Kats and P. Petrov, “Effect of curvature squared corrections in AdS on the viscosity of the dual gauge theory,” arXiv:0712.0743 [hep-th].
- [47] A. Buchel, R. C. Myers and A. Sinha, “Beyond eta/s = 1/4pi,” JHEP **0903** (2009) 084 [arXiv:0812.2521 [hep-th]].
- [48] M. Brigante, H. Liu, R. C. Myers, S. Shenker and S. Yaida, “The Viscosity Bound and Causality Violation,” Phys. Rev. Lett. **100** (2008) 191601 [arXiv:0802.3318 [hep-th]]. X. H. Ge and S. J. Sin, “Shear viscosity, instability and the upper bound of the Gauss-Bonnet JHEP **0905** (2009) 051 [arXiv:0903.2527 [hep-th]], X. H. Ge, S. J. Sin, S. F. Wu and G. H. Yang, “Shear viscosity and instability from third order Lovelock gravity,” Phys. Rev. D **80** (2009) 104019 [arXiv:0905.2675 [hep-th]]. X. H. Ge, Y. Matsuo, F. W. Shu, S. J. Sin and T. Tsukioka, “Viscosity Bound, Causality Violation and Instability with Stringy Correction and Charge,” JHEP **0810** (2008) 009 [arXiv:0808.2354 [hep-th]].